DOE-UCI-0003905

ULTRAFAST ELECTRON TRANSPORT ACROSS NANOGAPS IN NANOWIRE CIRCUITS

Final Technical Report

July 31, 2015

Eric O. Potma

University of California, Irvine
Department of Chemistry
Natural Sciences II
Irvine, CA 92697

DOE-UCI-0003905

ULTRAFAST ELECTRON TRANSPORT ACROSS NANOGAPS IN NANOWIRE CIRCUITS

Final Technical Report for the period April 2010 - April 2015

Date Issued/Published July 31, 2015

Eric O. Potma

PREPARED FOR THE UNITED STATES
DEPARTMENT OF ENERGY
OFFICE OF BASIC ENERGY SCIENCES

Work Performed Under Contract No. DE-SC0003905

1 Abstract/Program Scope

In this Program we aim for a closer look at electron transfer through single molecules. To achieve this, we use ultrafast laser pulses to time stamp an electron tunneling event in a molecule that is connected between two metallic electrodes, while reading out the electron current. A key aspect of this project is the use of metallic substrates with plasmonic activity to efficiently manipulate the tunneling probability. The first Phase of this program is concerned with developing highly sensitive tools for the ultrafast optical manipulation of tethered molecules through the evanescent surface field of plasmonic substrates. The second Phase of the program aims to use these tools for exercising control over the electron tunneling probability.

2 Technical Accomplishments

We have successfully accomplished the aims set out in Phase I and II. Below we summarize the main achievements that have been completed during the active period of the Program.

2.1 Phase I: Design and construction of an ultrafast microscope

Our proposed work relies on the ability to generate ultrafast laser pulses and to couple these into a two-dimensional electronic circuit with sub-micrometer precision. To enable the proposed work we have constructed a dedicated set-up using funds allocated to this Program. Our system includes a 2W Ti:sapphire laser (Coherent, Mira 900) pumped by a 10W frequency-doubled Nd:vanadate laser (Coherent, Verdi V10). The system produces a 2W pulse train at 800 nm with pulse widths of ∼150 fs. Our experiments require a second laser beam for dual-color pump-probe experiments. To generate the second color, we have built a tunable optical parametric oscillator. The system consists of a custom-designed, fanned periodically-poled LiNbO3 crystal. The layout of the system is shown in Figure 1. The system produces tunable pulses in the 950 nm to 1200 nm range, with a duration of 200 fs. Shorter pulses can be obtained by controlling the dispersion characteristics of the OPO cavity. The laser light source is coupled to an inverted microscope frame (Olympus, IX71), which is equipped with a CCD camera for capturing optical signals. This ultrafast microscope system is fully functional and is currently in use for our nanojunction pump-probe experiments.

2.2 Phase I: Launching of SPP modes in a circuit

In this Program, we proposed to use optically excited surface plasmon polarition (SPPs) modes to control the electron tunneling probability through a molecular conductor bridging two electrodes. The SPP modes have femtosecond temporal resolution and need to be directed accurately to the nanometer sized gap between the electrodes. One of the first targets in this Program is to demonstrate that such femtosecond modes can be launched into a two-dimensional circuit, and that their spatio-temporal propagation can be controlled.

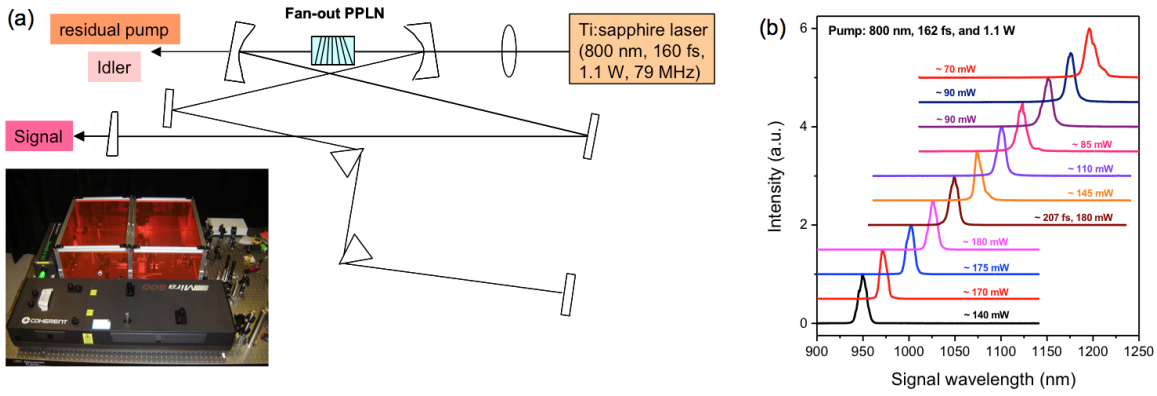

Figure 1: Custom-designed optical parametric oscillator (OPO). (a) Layout of the OPO. The inset shows a photo of the Ti:sapphire pump and the home-built OPO. (b) Output characteristics of the OPO. The system is continuously tunable from 950 to 1200 nm with powers in the 100 mW range (more than sufficient for our experiments).

We have successfully coupled freely propagating femtosecond pulses to propagating SPP modes in gold waveguides with a thickness of $\sim$ 30 nm. An example is shown in Figure (2), where a 240 fs pulse at 730 nm is coupled to a SPP mode that propagates into the gold extension. It can be seen through the leakage radiation that the SPP mode travels for more than 40 μm before it partially couples to the radiation field at the tip of the gold extension. These experiments show that femtosecond pulses can be conveniently coupled to SPP modes and transported over distances of more than 40 μm in the gold waveguide.

We have been able to couple a second fs-laser beam of a different color (935 nm) in the film. The presence of two SPP modes allows for wave-mixing experiments at locations far away from the laser spot. For this purpose, we have chosen to use CdSe quantum dots, which exhibit a strong fluorescence reponse, as a probe for the wave-mixing process. In Figure (2b), the four wave-mixing (FWM) signal at the laser spot is shown in addition to the two-photon excited fluorescence (TPEF) of a cluster of CdSe quantum dots, which are positioned near the tip of the waveguide.

Figure (3) shows that the two SPP of different frequencies can combined at the target to excite electronic transitions through nonlinear wave-mixing. The time-resolved TPEF signal shows a clear maximum when the two SPP modes overlap in time, indicating that dual-color wave-mixing occurred at the quantum dot. We have verified that the nonlinear signatures exhibit the correct dependence on the coupling angle and input polarization, which firmly confirm that nonlinear mixing of surface fields delivered by SPP wave-packets is responsible for the observed excitation mechanism. These experiments demonstrate that time-resolved femtosecond experiments can be performed at the distal site of a plasmonic waveguide. This assay decouples the required excitation energy from the residual illuminating photon flux, which is particularly important for the anticipated experiments involving plasmon controlled electron ejection at nanogaps.

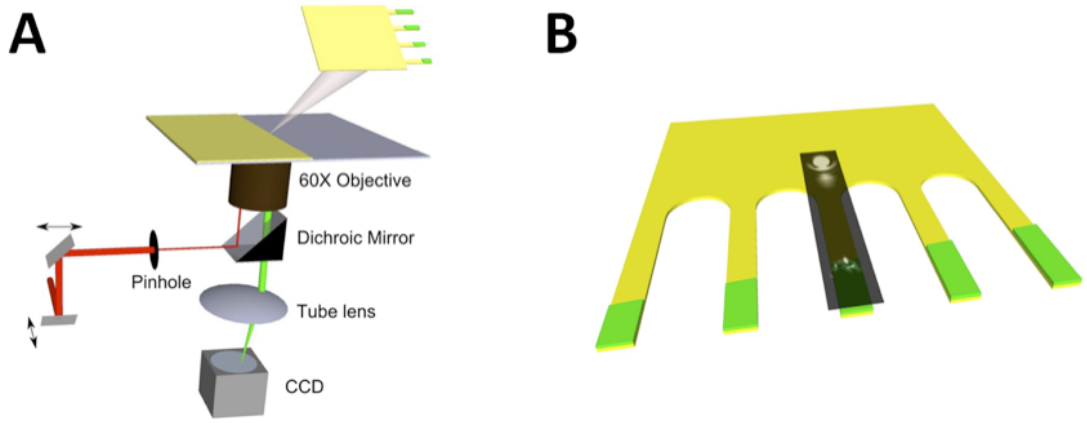

Figure 2: (A) Schematic of the experimental setup. (B) Sketch of the patterned gold film (yellow) with extensions partially covered with CdSe quantum dots (green). The overlaid image represents actual data showing the FWM signals at the laser spot and the TPEF of quantum dots.

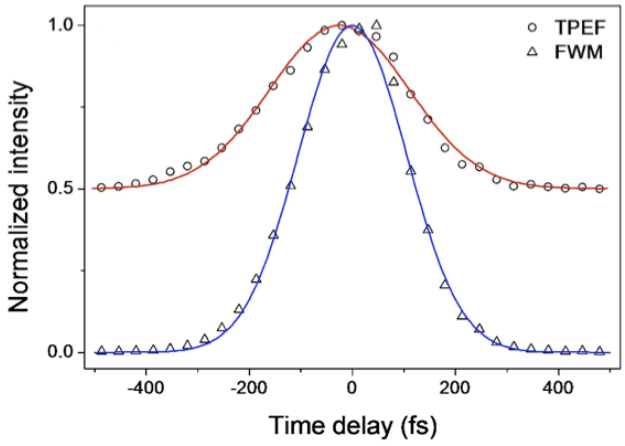

Figure 3: TPEF and FWM signals as a function of the time delay between the signal and idler beams. The red and blue curves show Gaussian estimates of the TPEF and FWM cross correlations, respectively.

2.3 Phase I: Controlling nonlinear interactions between the SPP mode and surface structures

After having established that SPP modes can be launched that that their energy content can be delivered to desired locations in the circuit, we tested the nonlinear light-matter interactions of the SPP pulse with selected materials on the surface. We have used the process of four-wave mixing (FWM) as a probe to test the nonlinear activity of the surface fields.

Using different excitation geometries, we have shown that femtosecond surface fields can efficiently drive nonlinear polarizations in nanoscopic structures on the surface.[1, 2] A counter-propagating excitation geometry is shown in Figure 4. We demonstrated that background-free, surface-sensitive $\chi^{(3)}$ signals can be generated from surface-bound structures and molecules in a controlled fashion.[3] We have also found that the surface plasmon fields enhance the $\chi^{(3)}$ response from such structures

by at least 100 times, relative to regular excitation conditions on a bare glass surface.

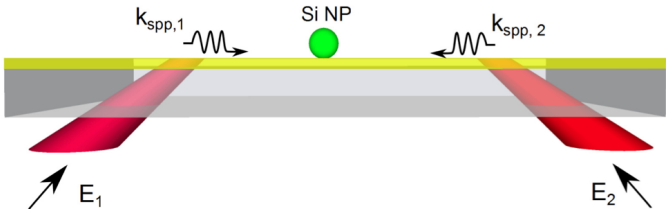

Figure 4: A scheme for the testing the ability of pulsed surface waves to generate optical nonlinearities in surface-bound objects. In this counter-propagating scheme, two femtosecond pulses are coupled into a 40 nm thick gold film at the Kretschman angle, generating two counter-propagating surface plasmon polariton waves. These pulsed surface waves can drive a nonlinear polarization in a probe particle (silicon nanoparticle). Strong, background-free FWM signals from the Si nanoparticle were observed.

2.4 Phase I: Lateral control of femtosecond SPP modes

The above-mentioned results are promising indicators that pulsed surface fields can be employed as actors in optical experiments of tethered molecules. However, the surface fields in these early experiments exhibited poor lateral confinement. Better control over the spatial properties of the pulsed plasmon waves is required to efficiently couple them into nanoscopic electrodes. Our first step in this direction is to focus the plasmon wave to a sub-micrometer spot, which improves the coupling efficiency into sub-wavelength waveguides. This approach can be compared, for instance, with focusing a freely propagating field into an optical fiber. For the purpose of plasmon focusing, we have fabricated Fresnel lenses in 40 nm gold surfaces. In order to test the ability of the focused surface fields to elicit nonlinear excitations, we have designed a dual Fresnel lens that yields two overlapping focal fields, which conveniently enables the generation of FWM signals.[4] An example is shown in Fig 5.

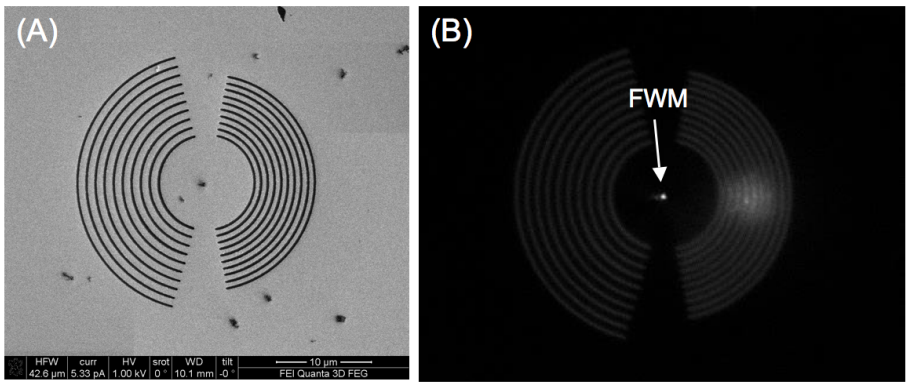

Figure 5: (A) SEM image of a dual Fresnel lens for plasmonic focusing. The lens consists of two halves with different periodic spacings of the grooves. The left half supports focusing of 820 nm light, while the right half support focusing of 720 nm light. A silicon nanoparticle is placed in the focal region for probing the ability of the focused surface waves to generate optical nonlinearities. (B) CCD image showing FWM of a Si nanoparticle upon focusing two femtosecond plasmon waves to the same sub-micrometer sized spot. A high FWM excitation efficiency is observed.

2.5 Phase II: Design and fabrication of nanojunctions

In Phase I we have established that a) femtosecond SPP modes can be launched in a 2D electronic circuit, b) the modes can be controlled and directed to desired locations in the circuit, and c) the nonlinear interaction between the SPP modes and molecular structures in the circuit can be controlled and measured. In Phase II, we have used these insights and applied them to the goal of controlling electron transfer through a bridging molecule in the circuit. The first aim in Phase II is to fabricate reproducible circuits with nano junctions. We have adopted the procedure for lithographically patterning tapered gold electrodes on a glass coverslip. This procedure yields patterned, 30 nm think gold films that hold six individual circuits. Each circuit consists of a source and a drain electrode, connected to external leads with spring-loaded pins mounted on a Teflon clamp, see Figure 6. To produce the nanojunction, the electrodes, which are initially connected, are separated by focused ion beam (FIB) milling. This procedure yields reproducible nanogaps in the 10 to 20 nm range. Junctions with inter-electrode spacings on the order of 10 nm show negligible tunneling currents in the open circuit. A negligible open circuit current is required for electron transport studies through molecular bridges. In addition, we have used use electromigration of partially milled junctions to generate nanogaps on the order of 2 to 5 nm. At these distances, tunneling currents can be observed. We have used this configuration to study plasmon-enhanced electron tunneling in open circuits.

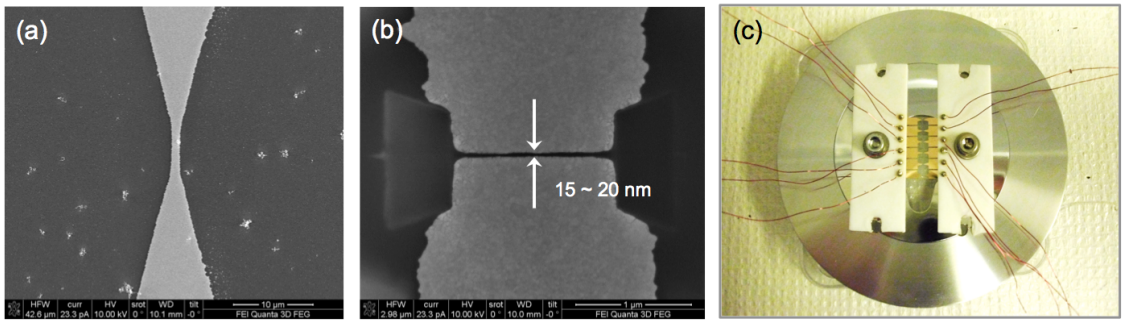

Figure 6: Circuit devices used for electron tunneling experiments. (a) Lithographically patterned bow-tie electrodes of a 0.170 mm borosilicate glass slide. Electrodes consist of a 30 nm layer of Au. (b) Formation of a nanojunction with focused ion beam milling. Reproducible gaps in the 10 nm range are obtained. (c) Packaging of six bow-tie electrode pairs on a single coverslip. Electrodes are connected with spring-loaded pins that are attached to leads.

2.6 Phase II: SPP-induced electron transfer across an engineered nano junction

Our second goal in Phase II is to control the tunneling of electrons across the junction with the help of femtosecond SPPs. Our approach is based on the excitation of a traveling SPP mode in the Au layer. To manage and suppress photon-induced heating of the junction, the SPP is excited at a remote location away from the junction. Subsequent propagation of the SPP towards the nano-gap enables manipulation of the surface field at the location of the junction. The changes in the electric field across the gap can induce tunneling of electrons, which can be be measured with a current meter. The basic layout of the experiment is shown in Figure 7b.

Figure 7c shows the dependence of the current across the gap as a function the input polarization of the laser light. A tunneling current is observed when the laser is P-polarized, while no current is flowing when the laser is S-polarized. *This experiment proves that the current is controlled exclusively by the surface field of the SPP mode*, as the SPP can only be excited with P-polarized light. This experiment proves unambiguously that controlled tunneling of electrons can be achieved across a nano-junction with femtosecond SPP wavepackets. Moreover, unlike previous work on light-induced tunneling, the tunneling currents here are stable, reproducible and measured under ambient temperatures and pressure.

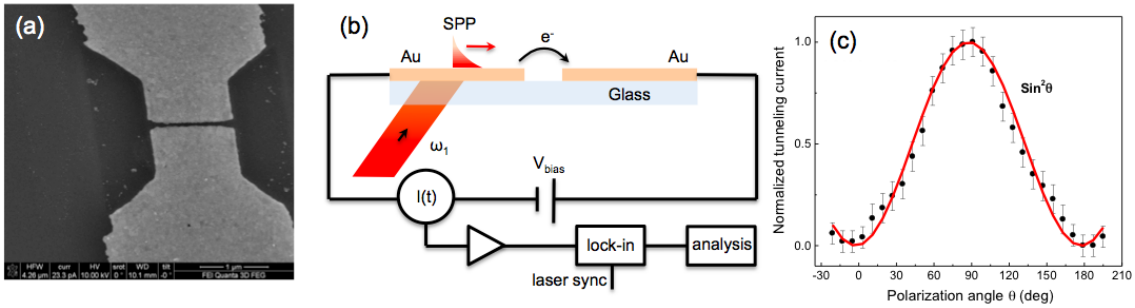

Figure 7: Femtosecond optical rectification in an open circuit. (a) Nanojunction prepared by partial FIB milling and electromigration. The effective gap size at the closest point in the junction is 8 nm. (b) Basic scheme for measuring the SPP induced current. (c) SPP-induced current as a function of laser input polarization. The polarization dependence confirms that the tunneling current is induced by the surface plasmon field.

We have characterized the open circuit SPP-induced electron current. We have found two regimes of induced electron currents, which we briefly summarize below.

- *SPP-induced electron transfer in the tunneling regime*
  Figure 8a depicts the I-V curve of the tunneling current for a fixed illumination power. The observed profile is indicative of electron tunneling mediated by the process of optical rectification. In this model, a dc current is generated by the ac surface field due to the second order nonlinearity of the junction. Such nonlinearities are the result of nanometer scale asymmetries in the gap. The red curve is a fit based on the optical rectification model. Further proof for this mechanism is provided by the dependence of the current on the light illumination power, illustrated by Figure 8b. At low excitation fields, the current is strictly linear with the incident power, as expected for the process of optical rectification.

  Electron tunneling mediated by optical rectification has been observed before, but never at *ambient pressures and temperatures*. In addition, these measurements are the first demonstration that dc currents can be generated with *femtosecond* temporal resolution, as electrons only flow across the junction during the elevated electric fields of the femtosecond SPP wave packet in the gap. One reason why these measurements are possible is that the remote SPP excitation scheme exhibits favorable heat dissipation characteristics which preserves the morphology of the junction and ensures stability of the measurements.

- *SPP-induced electron transfer in the field emission regime*
  As evidenced by Figure 8b, a different mechanism dominates the electron tunneling for stronger surface fields. The strong exponential power dependence is indicative of field electron emission as described by the Fowler-Nordheim equations. In this limit, the strong gradient

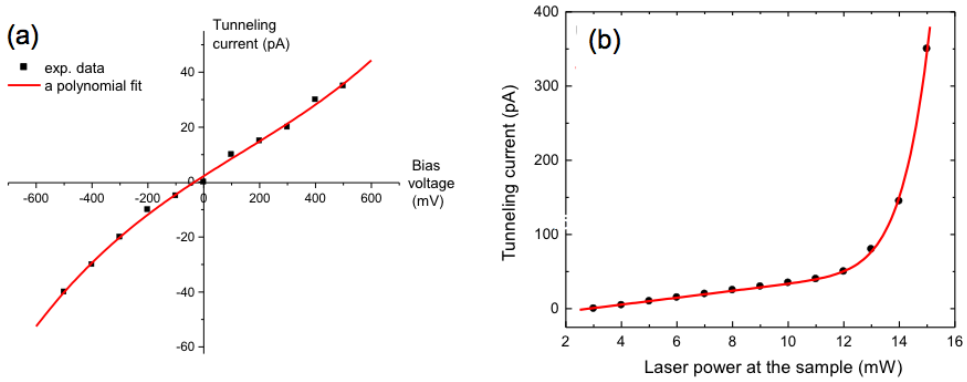

Figure 8: SPP induced current in an open circuit. (a) I-V curve in the limit of optical rectification. The current was measured for at a laser input power of 8 mW. (b) SPP induced current as a function of the laser input power. In the low power limit, optical rectification is the dominating process, while for higher SPP fields Fowler-Nordheim tunneling dominates. The red curve is a fit based on the combined effects of optical rectification and Fowler-Nordheim tunneling.

of the electric field in the gap narrows the tunneling barrier and thus increases the escape probability of electrons from the metal electrode. This is the first time that a clear transition between low field limit optical rectification and high field limit field electron emission is observed, which underlines the robustness and sensitivity of the SPP-based tunneling scheme developed in this Program.

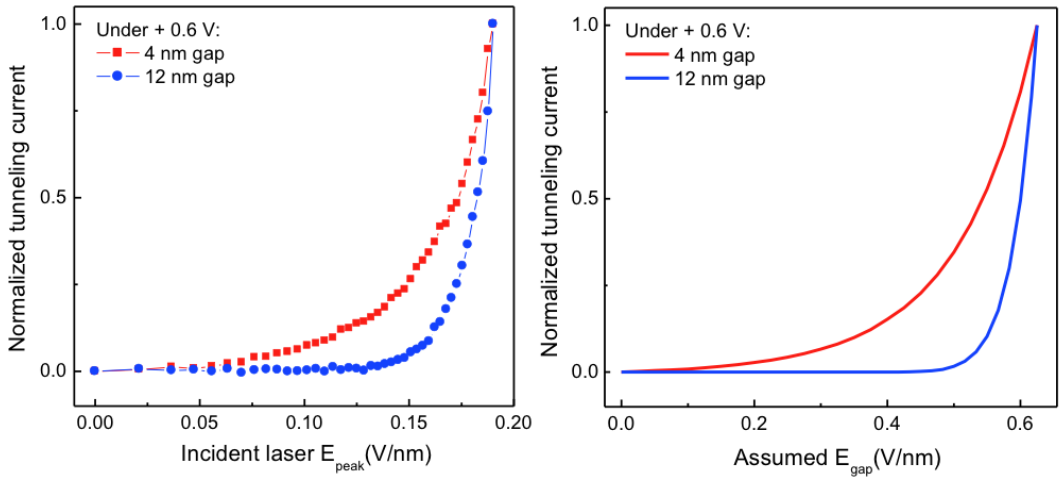

Figure 9: Dependence of electron current measured across a nano-junction as a function of laser field amplitude. Left panel: experiments for a 4 nm and a 12 nm gap. Right panel: simulations based on image potentials under the influence of ac modulation at optical frequencies. The difference between the 4 nm and the 12 nm is qualitatively reproduced.

2.7 Phase II: Mechanism of SPP-induced electron current across nm junctions

Figure 9 shows the electron current across the gap as a function of laser power. The current increases with higher illumination power. For a 12 nm gap, the profile is indicative of field emission of electrons. This process occurs when the field amplitude in the junction is high enough to significantly bend the potential, allowing electrons to tunnel to the altered barrier. The field emission process is independent of the size of the junction. For smaller gaps, like the 4 nm gap shown in red, a different profile is observed. The different dependence of the current with laser power reflects the transitional regime from field emission to electron tunneling.

We have developed a model for electron transport across nm-scale junctions.[6] The model retrieves Fowler-Nordheim type field emission in the large junction limit while predicting Tien-Gordon type rectification in the small junction limit. Importantly, this model is capable to explain electron currents in the intermediate regime between electron tunneling (<1 nm) and field emission, a regime not studied before. We observe that in gaps smaller than 5 nm, light can induce rectifying currents, where the magnitude of the current scales roughly linearly with the power of the incident light. Rectifying tunneling currents have been observed in sub-nm gaps, but have not been seen before in gaps larger than a nm. Our model establishes that for gaps smaller than 5 nm, the image potential is sufficiently bent in the presence of weak ac fields to allow linear rectification to occur. This new mechanism explains why efficient electron currents in sub 5 nm gaps can be observed. Electron currents in this regime are important, as junctions in this limit can be reliably fabricated with modern ion milling techniques. This regime is also relevant to chemistry, where junctions with bridging molecules are typically in the nm regime.

3 Future plans

In this Program we have demonstrated that femtosecond SPP modes can be launched in to an electronic circuit and tailored to control the electron current across an engineered nano gap. The SPP-induced current exhibits a distance-dependent tunneling component and a distance independent field emission component. Importantly, the open circuit currents generate here are stable and sustained over multiple hours under ambient conditions. The next step in this line of research is clear: bringing a bridging molecule into the nano gap and monitor the SPP-induced current through the molecular conductor. We have designed several circuits for this purpose. Our strategy is to separate the nano gap rectifier from the molecular conductor, and allocate these functional units to different parts of the circuit. In this scenario, the nano gap rectifier generates a femtosecond electron pulse, which propagates in the circuit (on ~ 100 μm distances before dispersion and attenuation) towards a molecular bridge, allowing clean pump-probe experiments with electron pulses on the single molecule conductor. Effectively, this new line of research marries the field of molecule electronics with a new capability: *femtosecond electronics*. The results acquired in the current program indicate that femtosecond electronics is possible, and show the way for exciting new possibilities for ultrafast molecular electronics. We are currently preparing a new proposal that focuses on this novel theme.

4 Expenditure of funds

We have received ARRA-related funds in the amount of $600,000 for year I–IV of the Program. These funds have been used to employ one postdoctoral fellow and one graduate student, who have been working full time on the project. By 01/01/14, these funds were fully outspent. On 08/22/13, we received Supplemental Funds in the amount of $48,859, which are allocated as equipment funds. By the 04/15/15, Supplement Funds is $25,249 were fully outspent. We have received the non-ARRA allocation of the budget in the amount of $150,000 for Year V, which has been used to support the postdoctoral fellow and the graduate student during the last year of the Program. As of 04/15/15, all funds have been fully outspent.

Publications with acknowledged DOE support:

[1] Y. Wang, X. Liu, D. Whitmore, W. Xing, and E. O. Potma, "Remote multi-color excitation using femtosecond propagating surface plasmon polaritons in gold films," *Opt. Express* **19**, 13454–13463 (2011).

[2] X. Liu, Y. Wang, and E. O. Potma, "Surface-mediated four-wave mixing of nanostructures with counterpropagating surface plasmon polaritons," *Opt. Lett.* **36**, 2348–2350 (2011).

[3] Y. Wang, X. Liu, A. R. Halpern, K. Cho, R. M. Corn, and E. O. Potma, "Wide field, surface-sensitive four-wave mixing microscopy of nanostructures," *Appl. Opt.*, **51** 3305–3312 (2012).

[4] X. Liu, Y. Wang, and E. O. Potma, "A dual-color plasmonic focus for surface-selective four-wave mixing," *Appl. Phys. Lett.* **101**, 081116 (2012).

[5] J. Brocious and E. O. Potma, "Lighting up micro-structured materials with four-wave mixing microscopy," *Materials Today* **16**, 344-350 (2013).

[6] B. Albee, X. Liu, and E. O. Potma, "Surface plasmon polariton-induced electron current across a nano gap," *submitted* (2015).

Invited presentations related to this Program:

Date	Title	Conference
01/05/2015	Femtosecond nanoscopy	Progress in Quantum Electronics, Snowbird, UT.
10/19/2014	Ultrafast electrical currents in nanojunctions	CPIMS Meeting, DOE, Washington, DC.
01/06/2014	Femtosecond microscopy in the single molecule limit	Progress in Quantum Electronics, Snowbird, UT.
10/29/2013	Four-wave mixing microscopy for material research	Materials Science and Technology, Montreal, ON.
08/26/2013	Surface sensitive coherent Raman scattering	Ultrafast Imaging and Spectroscopy, SPIE, San Diego, CA.
10/21/2012	Surface-sensitive nonlinear optical imaging	CPIMS, Department of Energy, Washington, DC.
01/24/2012	Surface-sensitive Four-wave Mixing Microscopy	Photonics West 2012, SPIE, San Francisco, CA.
01/05/2012	Surface-sensitive Four-wave Mixing Microscopy	Progress in Quantum Electronics, Snowbird, UT.
10/17/2011	Surface-sensitive Four-wave Mixing Microscopy	OSA Frontiers in Optics, OSA, San Jose, CA.
01/04/2011	Remote wave-mixing with surface plasmon polaritons	Progress in Quantum Electronics, Snowbird, UT.